Gain and Phase Error-Free LINC Transmitter

Xuejun Zhang and Lawrence E. Larson, *Fellow, IEEE*

***Abstract*—This paper presents a new correction technique for linear amplification with nonlinear components transmitters. During the transmit mode, the algorithm modulates and filters the baseband signal as a normal signal component separator, while during the correction mode, by use of a downconversion mixer, the gain and phase imbalance are measured and compensated by introducing a correction. This system is free of adjacent channel interference during the correction period. Analytical results and simulations demonstrate that this system is sufficient to suppress the out-of-band spectrum for mobile communications.**

***Index Terms*—Amplifier linearization, linear amplification with nonlinear components (LINCs), mobile communications, power amplifier.**

I. Introduction

THE OUTPHASED power amplifier concept dates back to the early 1930s as an approach for the simultaneous realization of high-efficiency *and* high-linearity amplification [1]. It has been revived recently for wireless communication applications under the rubric of linear amplification with nonlinear components (LINC) [2] and a variation known as CALLUM [3], [4]; many recent papers have developed the concept further [5]–[8]. The LINC concept takes an envelope modulated bandpass waveform and resolves it into *two* out-phased constant envelope signals, which are applied to highly efficient—and highly nonlinear—power amplifiers, whose outputs are summed. The advantage of this approach is that each amplifier can be operated in a very power-efficient mode, and the final output can be highly linear and free of intermodulation—a key consideration for bandwidth-efficient wireless communications. A block diagram of the approach is shown in Fig. 1.

One of the major disadvantages of this technique is the extremely tight tolerances on the matching of the two amplifier paths to achieve acceptably small out-of-band rejection. The out-of-band spectrum, created by the incomplete cancellation of the quadrature signal, strongly depends upon the modulation scheme as well as the rolloff factor of the shaping filter. Besides, it may also be affected by the ratio of the maximum input signal level to the signal level inside the signal component separator (SCS). Decreasing this ratio results in a higher requirement on the matching condition.

This problem has been analyzed by a number of authors [9]–[11], and the typical requirements for most practical applications are approximately 0.1–0.5 dB in gain matching or 0.4–2° in phase matching. This is nearly impossible to achieve in most practical situations, and several attempts have been made to correct for the errors through some kind of feedback approach. A "phase-only" correction was proposed in [9]. In this algorithm, the phase difference of two amplifier branches is used as a guide for the correction. The phase imbalance is detected by multiplying two amplifiers' outputs; hence, any imbalance after the power amplifiers is ignored. Besides, careful design is required to prevent the additional phase imbalance introduced by the measurement circuit. A simplex search algorithm was proposed in [10] to correct for both gain and phase errors. The correction of these errors relies on the measurement of the out-of-band emission, which requires a long data sequence for each iteration. This requirement sets a lower limit on the calibration time of approximate 1–2 s, which is a consideration in real-time applications. A direct search method was proposed in [12] to correct the gain imbalance as well as the consequent phase imbalance due to AM–PM transition. This technique is based on the evaluation of the in-band distortion by downconverting the LINC output and subtracting it from the input signal with an extra digital-to-analog (D/A) branch. The subtraction has to be quite accurate for the complete cancellation of the in-band signal.

The historical problems associated with this architecture, which these techniques address, have arisen because of the highly variable gain and phase response of the power amplifiers. What is required in order to minimize these effects is a relatively fixed standard of amplitude and phase that can be employed to *calibrate* each amplifier and then eliminate the effects of the errors. We will show how this fixed standard can reside *within* the amplitude and phase states of the digital I/Q modulators that feed the power amplifiers.

This paper will begin with a summary of the limitations of the LINC architecture in terms of gain and phase matching of the individual paths. That will be followed by a description of a new approach for calibrating and eliminating these errors at the baseband level. Simulation results will confirm the predictions of the new architecture. Finally, we will summarize some of the practical implementation issues involved with this architecture.

II. LINC Background and Architecture Limitations

The basic principle of LINC is to represent arbitrary bandpass signals by means of two out-phased constant envelope signals; these two signals are then amplified separately with a pair of highly nonlinear and power efficient amplifiers, and finally recombined through a passive combiner, as shown in Fig. 1. The separation of the bandpass signal is accomplished by the SCS. The detailed analysis of signal separation can be found in [11],

Manuscript received September 22, 1998; revised August 9, 1999. This work was supported by the U.S. Army Research Office under Multi-University Research Initiative Digital Communication Devices Based on Nonlinear Dynamics and Chaos.

The authors are with the Center for Wireless Communications, University of California–San Diego, La Jolla, CA 92093-0407 USA (e-mail: larson@ece.ucsd.edu).

Publisher Item Identifier S 0018-9545(00)08051-8.

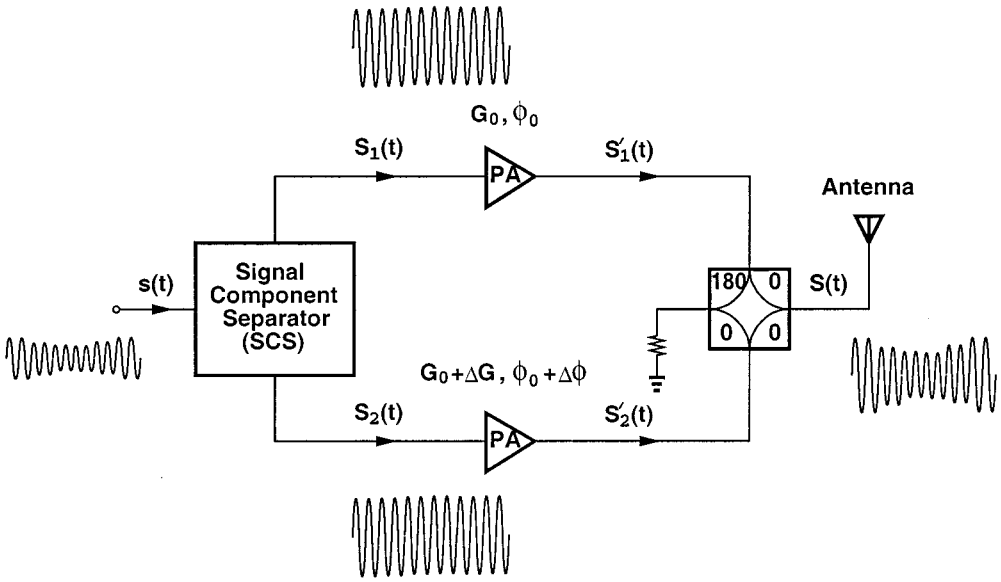

Fig. 1. Simplified LINC block diagram.

[13], and [14], and a brief mathematical description is given below.

A complex representation of the band-limited source signal can be written as

$$\boldsymbol{s}(t) = a(t)e^{j\theta(t)}; \qquad 0 \le a(t) \le V_m. \tag{1}$$

This signal is split by the SCS into two signals with modulated phase and constant amplitudes

$$\begin{aligned} S_1(t) &= \tfrac{1}{2}[\boldsymbol{s}(t) - \boldsymbol{e}(t)]_I \\ &= \tfrac{1}{2}V_m \cos[\theta(t) - \Psi(t)] \end{aligned} \tag{2a}$$

$$\begin{aligned} S_2(t) &= \tfrac{1}{2}[\boldsymbol{s}(t) + \boldsymbol{e}(t)]_I \\ &= \tfrac{1}{2}V_m \cos[\theta(t) + \Psi(t)] \end{aligned} \tag{2b}$$

where $\Psi(t) = \cos^{-1}[a(t)/V_m]$; "$I$" denotes the *in-phase* component. The quadrature signal $\boldsymbol{e}(t)$ is defined by

$$\boldsymbol{e}(t) = j\boldsymbol{s}(t)\sqrt{\frac{V_m^2}{a^2(t)} - 1}. \tag{3}$$

The two signals are then amplified individually and sent to a 180° hybrid combiner. Assuming no gain and phase mismatching, the in-phase signal components [$\boldsymbol{s}(t)$ in $\boldsymbol{S}_1'(t)$ and $\boldsymbol{S}_2'(t)$] add together and the out-of-phase signal components [$\boldsymbol{e}(t)$ in $\boldsymbol{S}_1'(t)$ and $\boldsymbol{S}_2'(t)$] cancel each other; the resultant signal is the desired amplified replica of the original signal

$$\begin{aligned} S(t) &= S_1'(t) + S_2'(t) \\ &= G_0 a(t) \cos[\theta(t) + \phi_0] \end{aligned} \tag{4}$$

where G_0 and ϕ_0 are the gain and the phase delay of the power amplifiers, respectively. The factor of $1/\sqrt{2}$ voltage reduction introduced by an ideal 180° hybrid combiner is neglected here for simplicity. If frequency translation is expected, two balanced quadrature modulators will be employed in amplifier branches following D/A converters to translate the baseband signal to the desired carrier frequency.

The above derivation is valid when the two power amplifier branches are well balanced, such that their gains and phase delays are exactly the same. Moreover, these balanced characteristics have to be maintained with variation of temperature and transition of channels. In practice, however, these conditions are difficult to achieve. In contrast to the narrow-band source signal $\boldsymbol{s}(t)$, the power spectrum of $\boldsymbol{e}(t)$ extends far into adjacent channels [10]. As a result, the incomplete cancellation of wide-band components leaves a residue in adjacent channels, introducing adjacent channel interference (ACI).

Another important source of ACI comes from the finite word length representation in the SCS, specifically, the quantization of the source signal prior to SCS and the quantization of the quadrature signal due to the D/A converters, although in both cases the quantization errors could be minimized and the desired out-of-band spectrum rejection could be achieved with a sufficiently long word length. The source signal quantization has a direct effect on the LINC output, which is an amplified replica of the quantized source signal. The quadrature signal quantization, on the other hand, introduces a variation to the constant envelope signals and hence amplifier gains, and finally produces gain mismatch. Readers may refer to [6] for a detailed analysis of source and quadrature signal quantization errors.

The imbalance in higher order nonlinear characteristics of the two power amplifiers may hurt the LINC amplifier's overall performance [11]. In the case of a narrow-band signal input, only the odd-order nonlinearity of the power amplifier may produce ACI. The result is gain compression, so the effect of odd-order distortion could be combined into gain imbalance consideration.

III. Calibration Technique for LINC Error Minimization

The improved LINC system makes use of the standard of amplitude and phase produced by the digital signal processor

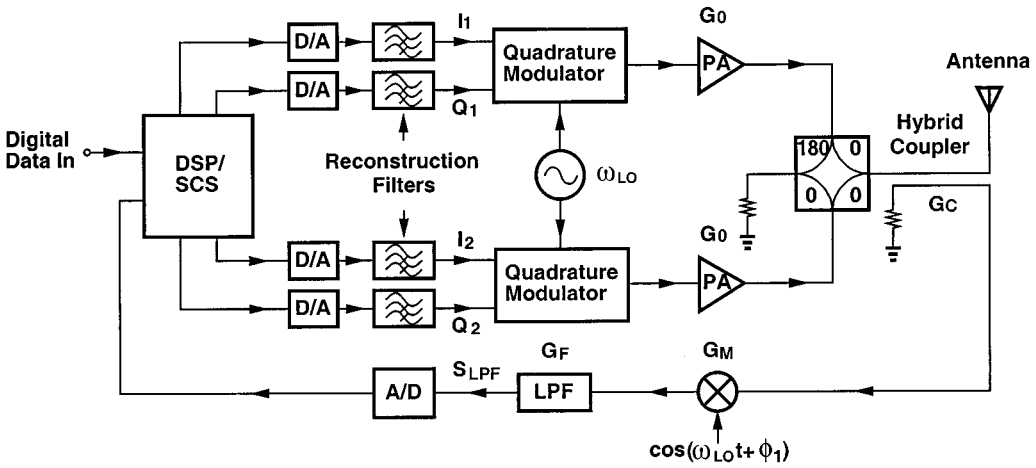

Fig. 2. LINC transmitter with correction loop.

(DSP) to calibrate the amplifiers. We first account for the gain and phase imbalance of the amplifiers and examine the LINC output signal. Suppose that the gain and phase imbalance of the lower amplifier with respect to the upper one are ΔG and $\Delta\phi$, respectively. Then, the LINC output will be

$$\begin{aligned} S(t) &= S_1'(t) + S_2'(t) \qquad (5a)\\ &= \tfrac{1}{2}G_0V_m\cos[\omega_c t + \theta(t) - \Psi(t) + \phi_0] \\ &\quad + \tfrac{1}{2}(G_0 + \Delta G)V_m \\ &\quad \cdot \cos[\omega_c t + \theta(t) + \Psi(t) + \phi_0 + \Delta\phi] \qquad (5b)\\ &= G_0\cos\left(\tfrac{1}{2}\Delta\phi\right)a(t)\cos\left[\omega_c t + \theta(t) + \phi_0 + \tfrac{1}{2}\Delta\phi\right] \\ &\quad + \tfrac{1}{2}\Delta G a(t)\cos[\omega_c t + \theta(t) + \phi_0 + \Delta\phi] \\ &\quad - G_0\sqrt{V_m^2 - a^2(t)}\sin\left(\tfrac{1}{2}\Delta\phi\right) \\ &\quad \cdot \cos\left[\omega_c t + \theta(t) + \phi_0 + \tfrac{1}{2}\Delta\phi\right] \\ &\quad - \tfrac{1}{2}\Delta G\sqrt{V_m^2 - a^2(t)}\sin[\omega_c t + \theta(t) + \phi_0 + \Delta\phi] \qquad (5c) \end{aligned}$$

where ω_c is the carrier frequency or channel center frequency. The difference between (5c) and (4) results from the amplitude and phase distortion of the summed output signal; the gain error modifies the output amplitude while the phase error modifies both. In the frequency domain, all four terms in (5c) contribute to the narrow-band signal, and the last two terms create undesired out-of-band spectrum. Roughly, the ACI is related to the ratio of the last two terms to the first two terms, which is proportional to the gain and phase imbalance. It is interesting to note that for signals with randomly varied amplitude and phase, the same amount of gain and phase error introduces approximately the same ACI.

The variables $a(t)$ and $\theta(t)$—which correspond to the baseband digital input modulated by the SCS—determine the relation between the four terms in (5c). Proper choice of $a(t)$ and $\theta(t)$ provides a mechanism to abstract the gain and phase error from the distorted output signal. Specifically, there are four unknowns—$\Delta G/G_0$, G_0, $\Delta\phi$, and ϕ_0—and two variables—$a(t)$ and $\theta(t)$—in (5c). Hence, four combinations of different $a(t)$ and $\theta(t)$ will be sufficient to determine the gain and phase errors. The proposed algorithm takes the approach of setting $a(t) = V_m$ or 0, and $\theta(t) = 0$ or $\pi/2$, corresponding to the I/Q components of $S_1(t)$ and $S_2(t)$ to be zero or $\pm V_m/2$, which is straightforward to realize with the SCS.

Furthermore, as we will demonstrate, the LINC output can be translated to baseband and allow a DSP correction algorithm to operate at the baseband frequency. As is illustrated in Fig. 2, a directional coupler withdraws a small portion of the LINC output and applies it to a mixer; downconversion is completed by the mixer, whose local oscillator frequency is the same as that of quadrature modulator. After low-pass filtering, the signal is then analog-to-digital (A/D) converted and sent to the DSP. The DSP determines the gain and phase error and eliminates the error effects by introducing a correction term. As a matter of fact, the DSP modulates and filters the original baseband signal and compensates the gain and phase imbalance—the SCS is part of its function. The following analysis illustrates the detailed derivation of this proposed algorithm.

Downconversion is accomplished by multiplying (5c) by $G_M\cos(\omega_c t + \phi_1)$, where G_M is the mixer gain and ϕ_1 is the phase difference between the local oscillator and the downconversion mixer. After passing it through a low-pass filter (LPF), the signal is then expressed as

$$\begin{aligned} S_{\mathrm{LPF}} &= \tfrac{1}{4}G_L V_m\cos[\theta(t) - \Psi(t) + \phi] \\ &\quad + \frac{1}{4}\left(1 + \frac{\Delta G}{G_0}\right)G_L V_m \\ &\quad \cdot \cos[\theta(t) + \Psi(t) + \phi + \Delta\phi] \qquad (6a)\\ &= \tfrac{1}{2}G_L\cos\left(\tfrac{1}{2}\Delta\phi\right)a(t)\cos\left[\theta(t) + \phi + \tfrac{1}{2}\Delta\phi\right] \\ &\quad + \frac{1}{4}\frac{\Delta G}{G_0}G_L a(t)\cos[\theta(t) + \phi + \Delta\phi] \\ &\quad - \tfrac{1}{2}G_L\sqrt{V_m^2 - a^2(t)}\sin\left(\tfrac{1}{2}\Delta\phi\right) \\ &\quad \cdot \cos\left[\theta(t) + \phi + \tfrac{1}{2}\Delta\phi\right] \\ &\quad - \frac{1}{4}\frac{\Delta G}{G_0}G_L\sqrt{V_m^2 - a^2(t)}\sin[\theta(t) + \phi + \Delta\phi]. \qquad (6b) \end{aligned}$$

Here G_L is the effective gain of the correction loop and consists of G_C (the gain of directional coupler), G_M, and G_F (the gain of LPF), i.e., $G_L = G_C G_M G_F$. ϕ denotes $\phi_L - \phi_1$, where ϕ_L indicates the phase delay of the whole correction loop from

output of the quadrature modulator to the input of the A/D converter.

The correction algorithm consists of several steps. First, we set the amplitude of the input baseband signal to the maximum allowable level of the SCS, i.e., $a(t) = V_m$. Consequently, the last two terms in (6b) disappear. Then, setting $\theta(t) = 0$, which means $I_1 = I_2 = V_m/2$ and $Q_1 = Q_2 = 0$, the result is

$$S_0 = \tfrac{1}{2}G'_L V_m \cos\left(\tfrac{1}{2}\Delta\phi\right)\cos\left(\phi + \tfrac{1}{2}\Delta\phi\right) - \frac{1}{4}\frac{\Delta G}{G_0}G_L V_m \sin\left(\frac{1}{2}\Delta\phi\right)\sin\left(\phi + \frac{1}{2}\Delta\phi\right) \quad (7)$$

where $G'_L = (1 + \Delta G/2G_0)G_L$. This result—$S_0$—is stored in the DSP. The next step in the algorithm involves setting $\theta(t) = \pi/2$ and keeping $a(t) = V_m$, corresponding to $I_1 = I_2 = 0$ and $Q_1 = Q_2 = -V_m/2$. Then

$$S_p = -\tfrac{1}{2}G'_L V_m \cos\left(\tfrac{1}{2}\Delta\phi\right)\sin\left(\phi + \tfrac{1}{2}\Delta\phi\right) - \frac{1}{4}\frac{\Delta G}{G_0}G_L V_m \sin\left(\frac{1}{2}\Delta\phi\right)\cos\left(\phi + \frac{1}{2}\Delta\phi\right). \quad (8)$$

Combining (7) and (8), the cosine and sine terms of $(\phi + \Delta\phi/2)$ are resolved approximately to be

$$\cos\left(\phi + \frac{1}{2}\Delta\phi\right) \simeq \frac{2}{G'_L V_m}S_0 - \frac{\Delta G}{G_0}\frac{G_L}{G'^2_L V_m} \cdot \frac{\sin(\Delta\phi/2)}{\cos^2(\Delta\phi/2)}S_p \quad (9a)$$

$$\sin\left(\phi + \frac{1}{2}\Delta\phi\right) \simeq -\frac{2}{G'^2_L V_m}S_p - \frac{\Delta G}{G_0}\frac{G_L}{G'_L V_m} \cdot \frac{\sin(\Delta\phi/2)}{\cos^2(\Delta\phi/2)}S_0 \quad (9b)$$

and further simplified to

$$\cos\left(\phi + \frac{1}{2}\Delta\phi\right) \simeq \frac{2}{G'_L V_m}S_0 \quad (10a)$$

$$\sin\left(\phi + \frac{1}{2}\Delta\phi\right) \simeq -\frac{2}{G'_L V_m}S_p \quad (10b)$$

since $\Delta G/G_0$ and $\Delta\phi$ are relatively small quantities.

We then set the amplitude of the input baseband signal to zero, i.e., $a(t) = 0$. Now, the first two terms in (6b) are removed. As before, we then set $\theta(t) = 0$, i.e., $I_1 = I_2 = 0$, $Q_1 = V_m/2$, and $Q_2 = -V_m/2$, to obtain S_a. Similarly, we set $\theta(t) = \pi/2$, i.e., $I_1 = V_m/2$, $I_2 = -V_m/2$, and $Q_1 = Q_2 = 0$, to obtain S_b. From (6) and (10), we may write S_a and S_b in matrix form as

$$\begin{pmatrix} S_a \\ S_b \end{pmatrix} = -\begin{pmatrix} -\cos\left(\tfrac{1}{2}\Delta\phi\right)S_p & S_0 \\ \cos\left(\tfrac{1}{2}\Delta\phi\right)S_0 & S_p \end{pmatrix}\begin{pmatrix} \dfrac{\Delta G/2G_0}{1+\Delta G/2G_0} \\ \sin\left(\tfrac{1}{2}\Delta\phi\right) \end{pmatrix}. \quad (11)$$

The above equation implies that the gain and phase errors are determined by S_0, S_p, S_a, and S_b. Fig. 3 illustrates their relationship in the case of small gain and phase imbalances, where S_a and S_b are the linear combinations of S_0 and S_p scaled by the gain and phase errors. Solving (11) for $\Delta G/G_0$ and $\Delta\phi$ yields

$$\begin{pmatrix} \dfrac{\Delta G/2G_0}{1+\Delta G/2G_0} \\ \sin\left(\tfrac{1}{2}\Delta\phi\right) \end{pmatrix} = -\frac{4}{G'^2_L V_m^2}\begin{pmatrix} -\dfrac{S_p}{\cos(\Delta\phi/2)} & \dfrac{S_0}{\cos(\Delta\phi/2)} \\ S_0 & S_p \end{pmatrix}\begin{pmatrix} S_a \\ S_b \end{pmatrix}. \quad (12)$$

For the gain error, we obtain

$$\frac{\Delta G}{G_0} = \frac{8}{G_L G'_L V_m^2 \cos(\Delta\phi/2)}(S_p S_a - S_0 S_b) \quad (13a)$$

$$\simeq \frac{8}{(G_L V_m)^2}(S_p S_a - S_0 S_b). \quad (13b)$$

Note that $G_0 V_m/2$ is actually the maximum signal level at the output of either power amplifier branch and $(G_0 V_m)^2/8$ might be referred to as the "average" power level normalized to a 1-Ω characteristic impedance. In the case of no gain or phase mismatch, the maximum signal at the output of the LPF is $G_L V_m/2$ from (6); hence we may define P_L as the average power level normalized to a 1-Ω characteristic impedance during calibration, i.e., $P_L = (G_L V_m)^2/8$. So we rewrite (13) as

$$\frac{\Delta G}{G_0} \simeq \frac{1}{P_L}(S_p S_a - S_0 S_b). \quad (14)$$

The estimation of the phase error according to (12) is given by

$$\sin\left(\frac{1}{2}\Delta\phi\right) = -\frac{4}{(G'_L V_m)^2}(S_0 S_a + S_p S_b) \quad (15)$$

and so

$$\Delta\phi \simeq -\frac{8}{(G'_L V_m)^2}(S_0 S_a + S_p S_b) \quad (16a)$$

$$\simeq -\frac{1}{P_L}(S_0 S_a + S_p S_b). \quad (16b)$$

As a conclusion, we only need to measure four signal values in order to estimate the gain and phase error. The approximations in (14) and (16) give rise to a certain amount of estimation error for the measurement of the gain and phase imbalance. Note that as long as the gain and phase error are close to zero, there will be little estimation error in (14) and (16). This implies that these approximations are effective in the sense that the estimate and compensation of gain and phase imbalance are iterative; with several iterations, the gain and phase error are able to converge to an arbitrarily low level. Checking (14) and (16), and in the case of small gain and phase error, neglecting the higher order terms, we immediately get

$$\left(\frac{\Delta G}{G_0}\right)_{\text{est}} \simeq \left(1 + \frac{\Delta G}{2G_0}\right)\left(\frac{\Delta G}{G_0}\right)_{\text{act}} \quad (17a)$$

$$(\Delta\phi)_{\text{est}} \simeq \left(1 + \frac{\Delta G}{G_0}\right)(\Delta\phi)_{\text{act}} \quad (17b)$$

where *est* and *act* indicate *estimate* and *actual*, respectively. The above equations conclude that after the first iteration, the actual gain error will be less than $\Delta G^2/(2G_0^2)$, while the actual

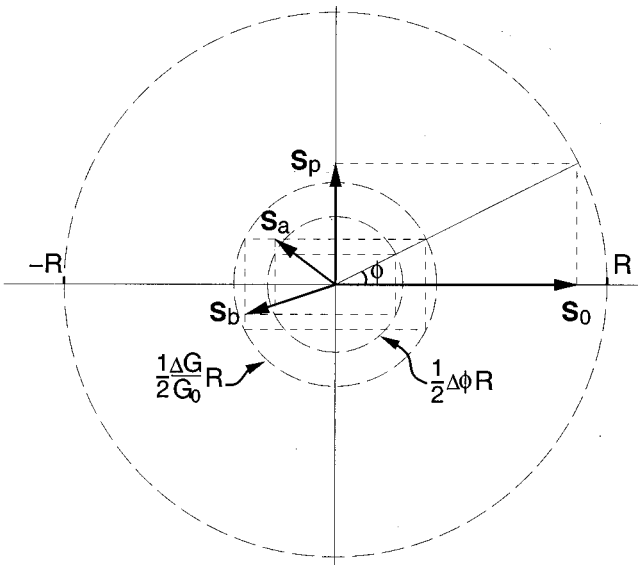

Fig. 3. Relationship between the gain/phase errors and four measured signals during calibration. The ϕ term represents the phase delay through the correction loop minus ϕ_1 of the downconversion mixer. $R = G_L V_m/2$.

phase error will be less than $\Delta\phi\Delta G/G_0$. Note that the iteration convergence is *independent* of the initial phase error. This is explained in accordance with (5); a 10% gain error is roughly equivalent to an 11.5° phase error. However, a 10% gain error will introduce a 5% estimation error in (14) and a 10% error in (16), whereas an 11.5° phase error will introduce at most 0.5% estimation error in (14) and 1% error in (16).

In order to estimate the gain and phase error by use of (14) and (16), we have to determine the average power of each amplifier P_L. That can be done by setting the lower amplifier branch signal level to zero, i.e., $I_2(t) = Q_2(t) = 0$. From (5a), we get the output signal

$$S = \tfrac{1}{2} G_0 V_m \cos[\omega_c t + \theta(t) - \Psi(t) + \phi_0]. \tag{18}$$

This signal is downconverted by the same mixer, A/D converted, and fed to the DSP. We set $a(t) = V_m$ and vary $\theta(t)$ as follows:

$$\theta = 0 \longrightarrow S'_{\mathrm{LPF}} = \tfrac{1}{4} G_L V_m \cos(\phi) \tag{19a}$$

$$\theta = \frac{\pi}{2} \longrightarrow S''_{\mathrm{LPF}} = -\frac{1}{4} G_L V_m \sin(\phi). \tag{19b}$$

Thus, the average power from the upper amplifier is given by

$$P_L = 2(S'^2_{\mathrm{LPF}} + S''^2_{\mathrm{LPF}}). \tag{20}$$

In practice, the dc offset of the LPF, mixer, and A/D converter will add to the signal as a constant background. To take this into account, we set $\theta(t) = -\pi/2$ and detect the signal level as usual. Comparing this value with (19b) will allow us to determine this constant background. Then we may subtract it from S'_{LPF} and S''_{LPF}.

With the estimation of gain and phase error at each iteration, the successive compensation is straightforward. We may accomplish the correction inside the DSP by scaling the signal level for gain error and introducing a phase delay for phase error in either amplifier branch. Specifically, $I_2(t)$ and $Q_2(t)$ are scaled by a factor of $1/(1+\Delta G/G_0)$ and delayed by $-\Delta\phi$. With $I_2(t)$ and $Q_2(t)$ specified by

$$I_2(t) = \tfrac{1}{2} V_m \cos[\theta(t) + \Psi(t)] \tag{21a}$$

$$Q_2(t) = -\tfrac{1}{2} V_m \sin[\theta(t) + \Psi(t)] \tag{21b}$$

we have

$$\begin{aligned} \hat{I}_2(t) &= \frac{1}{1+\Delta G/G_0} I_2(t)\cos(-\Delta\phi) \\ &\quad + \frac{1}{1+\Delta G/G_0} Q_2(t)\sin(-\Delta\phi) \\ &= \frac{1}{2}\frac{1}{1+\Delta G/G_0} V_m \cos[\theta(t) + \Psi(t) - \Delta\phi] \end{aligned} \tag{22a}$$

$$\begin{aligned} \hat{Q}_2(t) &= \frac{1}{1+\Delta G/G_0} Q_2(t)\cos(-\Delta\phi) \\ &\quad - \frac{1}{1+\Delta G/G_0} Q_2(t)\sin(-\Delta\phi) \\ &= -\frac{1}{2}\frac{1}{1+\Delta G/G_0} V_m \sin[\theta(t) + \Psi(t) - \Delta\phi]. \end{aligned} \tag{22b}$$

Here "^" means "corrected." After the quadrature modulator, we obtain

$$\begin{aligned} \hat{S}_2(t) &= \frac{1}{1+\Delta G/G_0} \hat{I}_2(t)\cos(\omega_c t + \phi_0) \\ &\quad + \frac{1}{1+\Delta G/G_0} \hat{Q}_2(t)\sin(\omega_c t + \phi_0) \\ &= \frac{1}{2}\frac{1}{1+\Delta G/G_0} V_m \\ &\quad \cdot \cos[\omega_c t + \theta(t) + \Psi(t) + \phi_0 - \Delta\phi]. \end{aligned} \tag{23}$$

At the end of the lower amplifier branch, the compensated signal then appears without the gain and phase imbalance, i.e.,

$$\hat{S}'_2(t) = \tfrac{1}{2} G_0 V_m \cos[\omega_c t + \theta(t) + \Psi(t) + \phi_0] \tag{24}$$

which is the ideal result. For simplicity, we assume a constant power gain for the lower amplifier. Since the algorithm is iterative, it will not lose generality for a nonlinear power amplifier, although it might be helpful to measure the gain as the function of power level as part of the correction algorithm.

IV. Simulation Results and Discussion

The above discussion suggests that it is necessary to build up a signal source, or an equivalent lookup table, as the fixed amplitude and phase standard within the DSP to determine the gain and phase imbalance. The error estimation and the data transmission cannot be processed by the DSP at the same time. We then say that there are two different working states for the transmitter: the "transmit" mode and the "correction" mode. Throughout the transmit mode, the DSP modulates and filters the baseband signal and operates like the normal SCS with the addition of the gain and phase error compensation. During the correction mode, the DSP measures the gain and phase imbalance and updates these values for compensation.

To achieve the desirable out-of-band spectrum suppression, it is essential to maintain two amplifier branches well balanced

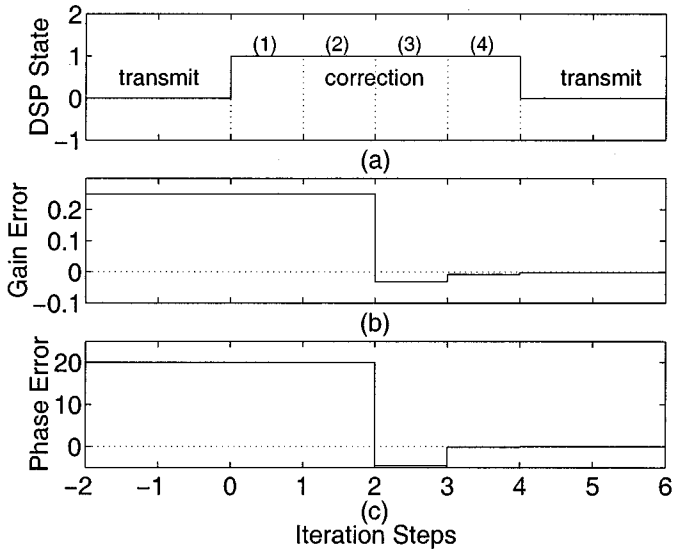

Fig. 4. Simulation results. (a) The DSP states; during the correction period, the DSP (1) calibrates P_L, (2)–(4) measures S_0, S_p, S_a, and S_b, calculates the gain and phase imbalance, and compensates the errors at the end of each iteration. (b) Actual gain error. (c) Actual phase error (degree) versus iteration steps ($\Delta G/G_0 = 25\%$, $\Delta\phi = 20^\circ$).

after correction. Intuitively, the correction can be done at the very start of transmission, before data transmission begins; this procedure, which is determined by the transient behavior of the LPF, may take tens of milliseconds or even less. In practice, the gain and phase characteristics of the power amplifier are highly variable due to thermal drift and component aging; moreover, these characteristics depend on the carrier frequency or channel. Thus, it is necessary to assign a specific time slot for the correction mode to allow the DSP to check the gain and phase imbalance and update this information regularly. This is easily achievable in most wireless systems that do not transmit on a continuous basis. For a further discussion of this issue, see Section V.

We simulated this new architecture with Cadence SPW according to the configuration of Fig. 2. An extra trigger input in this system is available to enable the DSP block to switch into the correction mode; as long as the compensated gain and phase error reduce to a preset allowable level, the DSP switches back to the transmit mode automatically. This procedure is illustrated in Fig. 4. In this example, the initial phase error is 20°, and the initial gain error is 25%. The allowable gain and phase error level was set to 0.5% (0.005 radian for phase error).

One example of the improvement achievable with this new technique is shown in Fig. 5. The modulation scheme used was quaternary phase-shift keying (QPSK), with a square-root raised cosine filter with rolloff factor of 0.4. The carrier frequency was chosen to be ten times higher than the symbol rate. The sampling frequency was 16 times higher than carrier frequency. The average power level from each amplifier was 20.3, and the dc offset of the LPF was 5.5.

From (14) and (16), we see that the measured gain and phase error are proportional to $1/P_L$, which suggests that a precise measurement of P_L is not essential, as long as we set a reasonably low level of the maximum allowable gain and phase error. We may need to estimate this parameter only once at the beginning of the calibration. Fig. 4(b) and (c) shows that the gain and phase error decrease rapidly with iteration steps. The error is nearly zero after four iterations. Note that the first iteration is assigned for the measurement and calibration of P_L. According to (17), the convergence of the algorithm, which is indicated by the maximum gain imbalance and the maximum phase imbalance after nth compensation, is given by

$$\left.\frac{\Delta G}{G_0}\right|_{\max_n} \simeq 2\left(\frac{\Delta G}{2G_0}\right)^{(2^n)} \tag{25a}$$

$$\left.\Delta\phi\right|_{\max_n} \simeq 2\Delta\phi\left(\frac{\Delta G}{2G_0}\right)^{(2^n-1)}. \tag{25b}$$

The gain error and phase error in Fig. 4(b) and (c), as expected from the above equations, were no more than ±3% and ±5° after the first compensation. Equation (25) also predicts that the gain and phase errors will be less than 0.05% and 0.08° after the second iteration, whereas the simulation shows that the actual gain and phase error are −0.8% and −0.11°, respectively. The discrepancy results from the approximation in (10). Nevertheless, except for the first correction period, the simulation results indicate that approximated three iteration steps are required for correction for each correction period.

Fig. 5 shows the corresponding output power spectrum of the LINC transmitter. Without correction, the ACI is around −22 dB, while with correction the out-of-band spectrum is suppressed efficiently below −74 dB. In this paper, the ACI is defined as the ratio of the peak spectral density of the residue outside the channel with respect to the peak spectral density of the modulation. Another simulation is shown in Fig. 6. The modulation scheme used is 16-QAM, with the same simulation conditions as the previous example. The ACI before and after correction is −19 and −71 dB, respectively.

It is also important to avoid ACI during the correction period. From (18), it is clear that during the calibration of P_L, the LINC output can be regarded as a phase modulated signal. The same thing happens when we fix the signal amplitude $a(t)$ and sweep

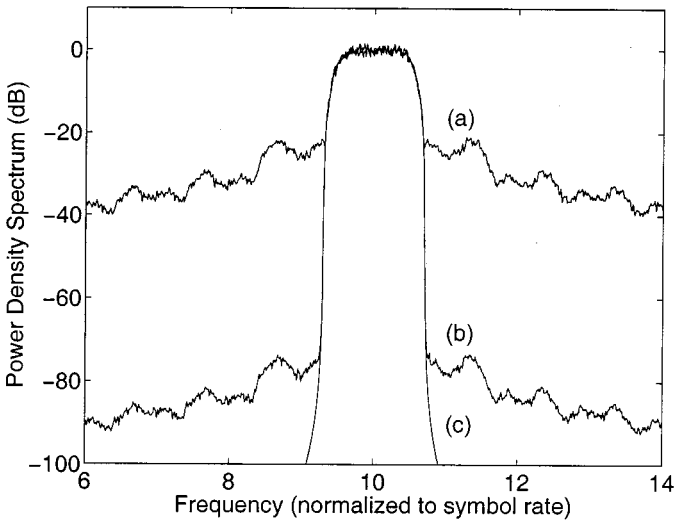

Fig. 5. Simulated LINC output spectrum for QPSK modulated data with square-root raised cosine filtering. (a) Wwithout correction, (b) with correction, and (c) without gain and phase imbalance ($\Delta G/G_0 = 25\%$, $\Delta\phi = 20°$).

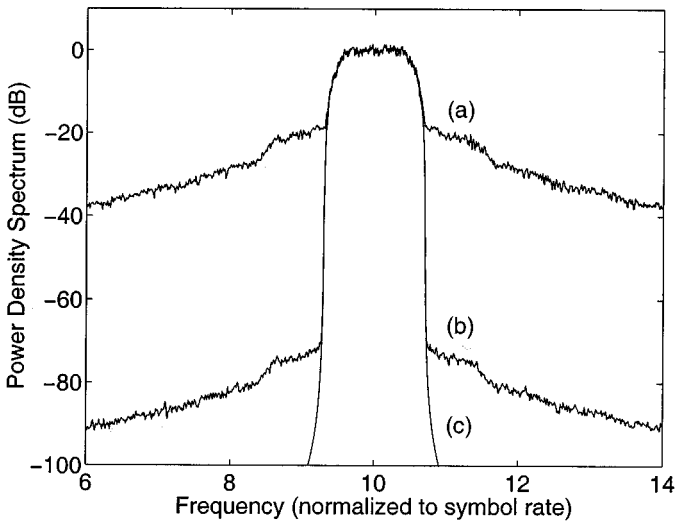

Fig. 6. Simulated LINC output spectrum for 16-QAM modulated data with square-root raised cosine filtering. (a) Without correction, (b) with correction, and (c) without gain and phase imbalance ($\Delta G/G_0 = 25\%$, $\Delta\phi = 20°$).

$\theta(t)$ according to (5c) in order to measure S_0, S_p, S_a, and S_b. The transmission bandwidth B_T of the PM signals is given by Carson's rule

$$B_T = 2(\beta + 1)B \tag{26a}$$

$$= 5.1B \tag{26b}$$

where β is the phase modulating index, in this case $\pi/2$, and B is the bandwidth of the modulating signal. When we fix $\theta(t)$ and vary the amplitude $a(t)$ from zero to V_m, and vice versa, the first two terms in (5c) are double sideband suppressed carrier (DSB-SC) signals, as are the last two terms in (5c). For this amplitude modulation, the output power spectrum is the linear translation of the modulating signal, and the bandwidth is not varied. Hence, the bandwidth of the LINC output is determined by the bandwidth of $a(t)$ and $\sqrt{V_m^2 - a^2(t)}$ and the amplitude ratio of the four terms in (5c). Thus, we are able to control the bandwidth of the LINC output by changing the variations of $a(t)$ and $\theta(t)$ during correction.

The quantization error of the A/D converter may limit the performance of the correction algorithm; hence the issue of the A/D converter dynamic range is important. By definition, the dynamic range is the ratio of the maximum detectable signal level to the minimum detectable level. For a $(B+1)$-bit A/D converter, we have

$$\Delta = \frac{X_m}{2^B} \tag{27}$$

where Δ and X_m are the step size and the full-scale level of the A/D converter, respectively. From (6) and (19), the maximum detectable signal level is $X_m = G_L V_m/2$. Due to the fact that the quantization error is not more than $\Delta/2$, we may write the worst case estimate of $\Delta\phi$ from (16) as

$$(\Delta\phi)_{\text{est}} = -\frac{8}{(G_L V_m)^2}\left[\left(S_0 + \frac{\Delta}{2}\right)\left(S_a + \frac{\Delta}{2}\right) + \left(S_p + \frac{\Delta}{2}\right)\left(S_b + \frac{\Delta}{2}\right)\right] \tag{28a}$$

$$\simeq (\Delta\phi)_{\text{act}} + \frac{\sqrt{2}}{2^B}\sin\left(\phi + \frac{1}{2}\Delta\phi - \frac{\pi}{4}\right). \tag{28b}$$

The above equation concludes that the estimation error $|\Delta\phi|_{\text{err}}$ of the phase imbalance is bounded by

$$|\Delta\phi|_{\text{err}} \le \frac{\sqrt{2}}{2^B}. \tag{29}$$

The similar result applies to the estimation error $|\Delta G/G_0|_{\text{err}}$ of the gain imbalance from (13)

$$\left|\frac{\Delta G}{G_0}\right|_{\text{err}} \le \frac{\sqrt{2}}{2^B} \tag{30}$$

Then the word length of the A/D converter is calculated to be

$$B + 1 = 1.5 - \frac{\log_{10}\delta}{\log_{10} 2} \tag{31}$$

with δ being the smaller value between the allowable gain and phase error. For the simulation in this paper, we set the maximum allowable gain and phase error to 0.5% and 0.29°. According to (31), $B + 1 = 10$ corresponds to the maximum allowable gain error of 0.28% and phase error of 0.16°. Hence, for the consideration of the A/D converter, a 10-bit word length representation is adequate to resolve the signal and achieve -60 dB ACI. This is easily achievable with modern A/D converter technology.

V. Limitation of the Correction Algorithm

As pointed out in the previous discussion, a dedicated time period is required to calibrate the system for adjustment of the gain and phase imbalances. This is a drawback compared to those techniques proposed in [9], [10], and [12], which operate during regular transmission. Despite this fact, this algorithm could be directly implemented to wireless systems that employ time-division duplex, e.g., digital European cordless telephone and personal handyphone systems, in which the calibration

could be processed when transmitter/receiver is off/on. This is not true for communications systems utilizing frequency-division multiplex. For time-division multiple access (TDMA), a certain short time period might be reserved to all users for calibration purpose only; utilizing other user's timeslots for calibration at specific frequency outside of the band is an alternative way. Another possible approach for TDMA or code-division multiple access systems might be to embed the calibration code at the beginning of each individual data packet, where the data packet is much longer than the calibration code because of the short calibration time. This requires a minor modification of the communication protocols.

So far, both the gain and phase compensation are accomplished by the DSP. Practically, a pair of highly nonlinear power amplifiers would be candidates to improve the energy efficiency of the overall system. In this case, there may be a problem for *gain error* compensation; it is difficult to adjust the gain of a nonlinear power amplifier while maintaining its high power efficiency. The optimum approach would be to "back off" the power amplifier with the *highest* output power until the two are equal. This would allow the power amplifier with the smaller output power to operate at peak efficiency.

Perfectly balanced quadrature modulators are assumed in this architecture, and that leads to another practical consideration. The quadrature errors (amplitude and phase) create a residue in the adjacent channels. To see how this would happen, we examine the LINC output in the presence of quadrature errors. The amplitude error g_1 and phase error δ_1 of the upper I/Q modulator are defined as follows:

$$S_1(t) = \tfrac{1}{2}V_m \cos(\omega_c t)\cos[\theta(t) - \Psi(t)] - \tfrac{1}{2}V_m(1+g_1)\sin(\omega_c t + \delta_1)\sin[\theta(t) - \Psi(t)]. \quad (32)$$

The output of the lower I/Q modulator—$S_2(t)$—has a similar expression. These two signals are then amplified separately and summed together to produce the final output. For the first-order approximation, we have

$$S(t) = S_1'(t) + S_2'(t) \quad (33a)$$

$$= (5c) - \tfrac{1}{2}G_0(g_1+g_2)a(t)\sin[\theta(t)]\sin(\omega_c t + \phi_0) - \tfrac{1}{2}G_0(\delta_1+\delta_2)a(t)\sin[\theta(t)]\cos(\omega_c t + \phi_0) + \tfrac{1}{2}G_0(g_1-g_2)\sqrt{V_m^2 - a^2(t)}\cos[\theta(t)]\sin(\omega_c t + \phi_0) + \tfrac{1}{2}G_0(\delta_1-\delta_2)\sqrt{V_m^2 - a^2(t)}\cos[\theta(t)]\cos(\omega_c t + \phi_0). \quad (33b)$$

It is clear that the $a(t)$ terms are narrow band and introduce in-band distortion—hence the intersymbol interference, while $\sqrt{V_m^2 - a^2(t)}$ terms are wide band and create the out-of-band spectrum. The above equation demonstrates that the out-of-band spectrum can only be suppressed by matching the two amplitude errors and the two phase errors of the I/Q modulators, not by adjusting the gain and phase delay of the amplifier branch.

On the other hand, the presence of the quadrature errors degrade the measurement accuracy of the gain and phase imbalances. Following similar procedures used to derive the signal after the LPF, it is not difficult to obtain the following expressions by use of (14), (16), and definitions of S_0, S_p, S_a, and S_b

$$\left(\frac{\Delta G}{G_0}\right)_{est} = \left(\frac{\Delta G}{G_0}\right)_{act} - (g_1 - g_2)\sin^2\phi - (\delta_1 - \delta_2)\sin\phi\cos\phi \quad (34a)$$

$$(\Delta\phi)_{est} = (\Delta\phi)_{act} - (\delta_1 - \delta_2)\cos^2\phi - (g_1 - g_2)\sin\phi\cos\phi. \quad (34b)$$

Note that above equations are consistent with (17) in the sense of the first-order approximation. The measured gain and phase imbalances are constantly offset by certain small amount, depending on the quadrature errors and phase delay of the correction loop. As a result, the gain and phase errors will finally reach

$$\left.\frac{\Delta G}{G_0}\right|_{n\to\infty} = (g_1 - g_2)\sin^2\phi + (\delta_1 - \delta_2)\sin\phi\cos\phi \quad (35a)$$

$$\Delta\phi|_{n\to\infty} = (\delta_1 - \delta_2)\cos^2\phi + (g_1 - g_2)\sin\phi\cos\phi. \quad (35b)$$

An interesting observation resulting from (33) and (34) is that as long as the amplitude errors and phase errors of two I/Q modulators are matched, the gain and phase imbalances between amplifier branches are measured accurately and can be reduced to an arbitrarily low level. Furthermore, no out-of-band spectrum is created.

In a word, the quadrature errors set a limit for the LINC overall performance. Fortunately, highly accurate quadrature modulators are now routinely available for upconversion and downconversion applications [15], with gain and phase accuracy within the requirements of this proposed algorithm.

VI. Conclusion

We have presented a calibration technique for iterative correction of the gain and phase errors of the LINC transmitter. This scheme relies on the fixed standard of amplitude and phase stored in the DSP to calibrate the gain and phase errors of the nonlinear power amplifiers. The simplicity of this scheme comes from the fact that only four signal values are required to completely determine these errors at each iteration. The practical considerations of the implementation of this scheme are addressed, including the convergence of this algorithm, the dc offset, the bandwidth requirement during correction period, the quantization error of the A/D converter, and the quadrature errors of the I/Q modulators. The typically small quadrature errors determine the limit of the LINC overall performance. Simulation results confirm the analytical predictions and demonstrate that this system is sufficient to suppress the out-of-band spectrum for mobile communication applications.

References

[1] H. Chireix, "High power outphasing modulation," *Proc. IRE*, vol. 23, pp. 1370–1392, Nov. 1935.

[2] D. C. Cox, "Linear amplification with nonlinear components," *IEEE Trans. Commun.*, vol. COM-23, pp. 1942–1945, Dec. 1974.

[3] K. Y. Chan, A. Bateman, and M. Li, "Analysis and realization of the LINC transmitter using the combined analogue locked loop universal modulator CALLUM," in *Proc. IEEE 44th Veh. Technol. Conf.*, vol. 1, Stockholm, Sweden, June 8–10, 1994, pp. 484–488.

[4] K. Y. Chan and A. Bateman, "Analytical and measured performance of the combined analogue locked loop universal modulator CALLUM," *Proc. Inst. Elect. Eng. Commun.*, vol. 142, no. 5, pp. 297–306, Oct. 1995.
[5] F. H. Raab, "Efficiency of outphasing RF power-amplifier systems," *IEEE Trans. Commun.*, vol. COM-33, pp. 1094–1099, Oct. 1985.
[6] L. Sundstrom, "The effect of quantization in a digital signal component separator for LINC transmitters," *IEEE Trans. Veh. Technol.*, vol. 45, pp. 346–352, May 1996.
[7] ——, "Effects of reconstruction filters and sampling rate for a digital signal component separator on LINC transmitter performance," *Electron. Lett.*, vol. 31, no. 14, pp. 1124–1125, July 6, 1995.
[8] L. Sundstrom and M. Johansson, "Effect of modulation scheme on LINC transmitter power efficiency," *Electron. Lett.*, vol. 30, no. 20, pp. 1643–1645, Sept. 29, 1994.
[9] S. Tomisato, K. Chiba, and K. Murota, "Phase error free LINC modulator," *Electron. Lett.*, vol. 25, no. 9, pp. 576–577, Apr. 27, 1989.
[10] L. Sundstrom, "Automatic adjustment of gain and phase imbalances in LINC transmitters," *Electron. Lett.*, vol. 31, no. 3, pp. 155–156, Feb. 2, 1995.
[11] F. Casadevall and J. J. Olmos, "On the behavior of the LINC transmitter," in *Proc. 40th IEEE Veh. Technol. Conf.*, Orlando, FL, May 6–9, 1990, pp. 29–34.
[12] S. Ampem-Darko and H. S. Al-Raweshidy, "Gain/phase imbalance cancellation technique in LINC transmitters," *Electron. Lett.*, vol. 34, no. 22, pp. 2093–2094, Oct. 1998.
[13] L. Couch and J. L. Walker, "A VHF LINC amplifier," in *Proc. IEEE Southeastcon'82*, Destin, FL, Apr. 4–7, 1982, pp. 122–125.
[14] S. A. Hetzel, A. Bateman, and J. P. McGeehan, "LINC transmitter," *Electron. Lett.*, vol. 27, no. 10, pp. 844–846, May 9, 1991.
[15] I. A. Koullias, J. H. Havens, I. G. Post, and P. E. Bronner, "A 900-MHz transceiver chip set for dual-mode cellular radio mobile terminals," in *ISSCC Dig. Tech. Papers*, Feb. 1993, pp. 140–141.

Xuejun Zhang received the B.S. degree in semiconductor physics from Peking University, China, in 1991 and the M.S. degree in electrooptics from the National University of Singapore, Singapore, in 1997. He is currently pursuing the Ph.D. degree in electrical engineering at the University of California–San Diego.

He was with Southwestern Computing Center, China, from 1991 to 1992 and the Institute of Applied Electronics of the China Academy of Engineering Physics, China, from 1992 to 1995, where he was involved in various research projects, including laser optics, optical diagnostic system, nonlinear optics, and optical materials. His research interests include RF power amplifiers and power amplifier linearization techniques.

Lawrence E. Larson (S'83–M'86–SM'90–F'99) received the B.S. degree in electrical engineering and the M.Eng. degree from Cornell University, Ithaca, NY, in 1979 and 1980, respectively. He received the Ph.D. degree in electrical engineering from the University of California–Los Angeles in 1986.

He joined Hughes Research Laboratories in Malibu, CA in 1980, where he directed work on high-frequency InP, GaAs, and silicon integrated circuit development for a variety of radar and communications applications, as well as MEMS-based circuits for RF and microwave applications. He was also Assistant Program Manager of the Hughes/DARPA MIMIC Program from 1992 to 1994. From 1994 to 1996, he was with Hughes Network Systems, Germantown, MD, where he directed the development of radio-frequency integrated circuits for wireless communications applications. He joined the faculty at the University of California–San Diego in 1996, where he is the inaugural Holder of the Communications Industry Chair. He has published more than 100 papers and has received 21 U.S. patents.

Dr. Larson is a member of Sigma Xi and Eta Kappa Nu. He was a corecipient of the 1996 Lawrence A. Hyland Patent Award of Hughes Electronics for his work on low-noise millimeter-wave HEMT's.